

SHORT COMMUNICATION

Radiomics: Phases of osteoclastic metastasis status in breast cancer identified by morphologic markers

Valentin Steinhauer^{1*}  **and Nikolay I. Sergeev^{2,3}** 

¹Department of Telecommunications, Devoteam GmbH, Weiterstadt, Hessen, Germany

²Russian Scientific Center of Roentgenoradiology, Russian Research Center of Roentgenology and Radiology of the Ministry of Health of the Russian Federation, Moscow, Russia

³Department of Radiology, Pirogov Russian National Research Medical University, Moscow, Russia

(This article belongs to the *Special Issue: Advances in Bone Metastasis Management*)

Abstract

In the practical work of radiologists or oncologists, particularly in individualized treatment, a rapid and accurate diagnosis, timely assessments of drug effects, and direction of disease progression are essential. Radiomics and neural networks offer significant help in analyzing data from diagnostic imaging studies. This study examines quantitative biomarkers derived from magnetic resonance imaging, tentatively categorized as mathematical morphological markers, and explores their relationship with osteoclast tumor regression in breast cancer. This study aims to determine the consistency of imaging biomarkers in the stabilization, healing, and progression of breast cancer bone metastases.

Keywords: Radiomics; Neural networks; Osteoclastic metastases; Magnetic resonance imaging; Time sequences of biomarkers; Radial basis function

*Corresponding author:

Valentin Steinhauer
(valentin.steinhauer@t-online.de)

Citation: Steinhauer V, Sergeev NI. Radiomics: Phases of osteoclastic metastasis status in breast cancer identified by morphologic markers. *Cancer Plus*. 2025;7(1):109-115. doi: 10.36922/cp.6649

Received: November 28, 2024

Revised: January 07, 2025

Accepted: February 26, 2025

Published online: March 21, 2025

Copyright: © 2025 Author(s). This is an Open-Access article distributed under the terms of the Creative Commons Attribution License, permitting distribution, and reproduction in any medium, provided the original work is properly cited.

Publisher's Note: AccScience Publishing remains neutral with regard to jurisdictional claims in published maps and institutional affiliations.

1. Introduction

The primary goal of breast cancer treatment is the reliable evaluation of its effectiveness, focusing on the earliest possible detection of disease stabilization or progression criteria, which allows timely adjustment of the therapy plan.¹ Using radiomics offers significant opportunities for enhancing disease control through imaging methods, particularly image processing, whose full capabilities remain underutilized.² The challenges of the widespread application of radiomics include insufficient theoretical developments, difficulties in correlating identified features with clinical manifestations and morphological data, image artifacts, and image normalization, among others.³⁻⁵ The prolonged course of bone metastases creates a pathological cycle in which osteoclasts stimulate increased activation of osteoblasts. In parallel, these processes are further influenced by treatment, and from a conventional diagnostic perspective, they appear as numerous mixed areas. According to multi-slice spiral computed tomography (CT) data, metastases are defined by the alternation of fragments of compaction and rarefaction. On magnetic resonance imaging (MRI), they appear as diffuse, heterogeneous zones of peritrabecular edema, while positron emission tomography reveals multiple small

merging foci with varying standardized uptake values.⁶⁻⁸ In these cases, dynamic analysis of imaging studies is crucial, as visual assessment by a radiologist alone may be insufficient in the absence of obvious signs of progression. Therefore, effective treatment monitoring now relies on advanced machine-based analysis to identify imaging biomarkers that correspond to phase changes in the metastatic process.

The study aims to examine the relationship between radiomic imaging biomarkers and the stages of osteoclastic metastasis development processes.

2. Methods

2.1. Clinical characteristics

The MRI images were obtained from three patients diagnosed with breast cancer initial states T2N2-3M1, who underwent comprehensive treatment, including neoadjuvant chemotherapy, mastectomy, and adjuvant chemotherapy combined with remote radiation therapy at doses up to 56 Gy. The patients are referred to as Spine-2 (three scans) and Spine-3 (four scans). In addition, in one case, called Spine-1 (12 scans starting from the initial state), CDK 4/6 inhibitors – palbociclib and abemaciclib – along with radiation therapy were used. According to diagnostic methods (biopsy), metastatic skeletal involvement was confirmed in all patients. After the diagnosis was established, foci in the spine were further monitored using MRI with intravenous contrast enhancement with gadolinium-based preparations. Follow-up intervals were approximately 3 months, with each patient undergoing a minimum of three MRI scans and a maximum of 12 scans. Osteoscintigraphy and CT served as conventional reference methods for comparison.

The control group consisted of 10 MRI images of healthy spines without fractures, and the patients' age range was 27 – 55 years.

2.2. Modeling of the radiomics process

The workflow consisted of two primary stages: Evaluation of diagnostic images by a radiologist and machine-based analysis. To objectivize the results, all data were anonymized, and observations were assigned conditional labels (i.e., Spine-1, Spine-2, and Spine-3), followed by the corresponding study sequence. Notably, both evaluation processes proceeded in parallel, generating a report, in which the final diagnosis had a three-digit scale: Improvement, stabilization, and progression.

The software used in this study included both proprietary modules and modules from well-known libraries, which are summarized in DICOM Viewer. Programming was

conducted in the JAVA/JAVAFX language, which is characterized by high portability, sufficient processing speed, and extensive graphical and computational capabilities. The experimental system was implemented as a separately installed program module named “Radiomica Applicata.” For DICOM data processing, the DICOM software library⁹ was used. The user interface has a classical structure: a menu at the top, an image tree on the left, and images on the right. The operation is the same as in the standard DICOM Viewer. To automate phase detection, a radial basis function neural network was used.¹⁰

2.2.1. Morphological markers and their time sequences

Earlier studies analyzing MRI and CT tomograms with bone metastases^{11,12} have identified three radiomics and morphologic biomarkers: Arcela, Caldera, and Contrast. Their definitions are given as follows:

1. Arcela: This operator evaluates the complexity of an image, where one image is considered more complex than another if the sum of the boundaries of its constituent objects is larger
2. Caldera: Caldera: In breast cancer, many structures in bone have radial symmetry,¹³ as seen not only in metastases but also in inflammatory foci and “sclerosing” zones induced by them. The caldera varies in intensity relative to the intervertebral disc (black, white, and ISO). If the intensity of the Caldera is lower than the intensity of the intervertebral disk, the Caldera is labeled as black
3. Contrast: It is widely known for its application in imaging. Therefore, we propose using contrast accumulation dependence as a marker of disease progression in our software package as well.

2.2.2. Hilliness

In this study, the software package utilized the aforementioned biomarkers: Arcela for tracking image complexity, Contrast for measuring changes in contrast accumulation, and Caldera for detecting radially symmetrical objects. However, during disease regression, a point may be reached where these changes become insignificant, necessitating more subtle and targeted markers than the MD Anderson criteria and response evaluation criteria in solid commonly used clinically. For example, this is applicable in the “healing” phase, which can be interpreted in a first approximation as wound healing, that is, as a stage of growth of loose fibrous connective tissue. Although the fibrous structure is hardly detectable by the existing devices, its appearance and development are reflected in changes in the relief of image intensity. During tumor regression, tissues

gradually change their texture, returning to the original state, though not exactly replicating it. Vertebrae of young and healthy individuals display a faint “noise” in relief in sagittal projection, corresponding to the trabecular structure. With age, this “hilliness” increases due to osteoporosis. However, the intensity of relief exhibits less variation in heights and depressions compared to the disease period. To quantify these variations, we define hilliness as the standard deviation from the mean intensity in the region of interest (ROI), normalized by the mean intensity in the ROI.

3. Results

3.1. Using hilliness as a morphological marker

Before exploring the relationship between all the developed markers, is important to note, that the functionality of hilliness fits well into the Hanahan and Weinberg scheme¹⁴ of important cancer traits based on object complexity.

From the results of time sequences based on hilliness in the Spine-1 observation, diffuse metastatic bone lesions led to a generalized decrease in bone marrow signal intensity (discs on T1 and T2-weighted images appear brighter than bones). The time sequence of changes in the Th7 vertebra is displayed in Figure 1. Here, the general stabilization of intensity against a background of decreasing fluctuations over time, which is a characteristic of healing wounds, is visible. To visualize changes over time, the program module can plot a graphical curve depending on the biomarker type.

A more detailed analysis of Spine-1 (thoracic spine) over 12 studies revealed that the contrast agent initially accumulates distinctly in the nidus, followed by the introduction of palbociclib and its accumulation in the surroundings. The Arcela marker, which measures image complexity and is associated with chaotic angiogenesis in the nidus, performs well during this period. In addition, the curve displays variations in the mean ROI intensity, corresponding to the withdrawal of palbociclib and the switch to abemaciclib.

Reduced complexity in the lytic focus was also observed in T1 at hypointensity. The increase in complexity (i.e., the increase in the sum of object boundaries) with the positive effect of therapy, such as palbociclib, grows rapidly, enabling the physician to ensure the effectiveness of the medication within the first 3 months. Further Caldera values decrease and Hilliness becomes more prominent. Caldera values decrease and Hilliness becomes more prominent. Over time, as intensity stabilizes the variance of deviations from the mean intensity decreases and eventually stabilizes in the Th7 vertebra (Figure 2).

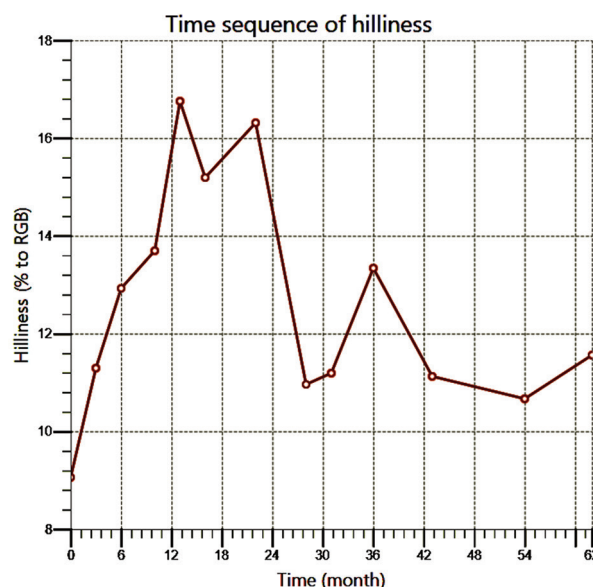


Figure 1. Hilliness of lytic metastasis without contrast agent accumulation.

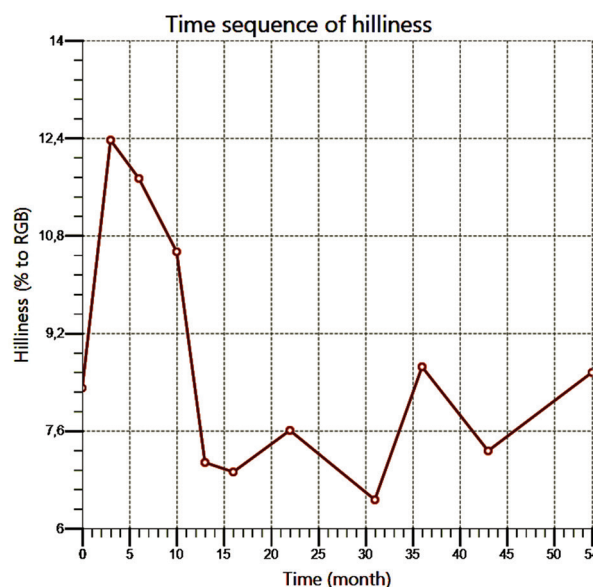


Figure 2. Hilliness of lytic metastasis with contrast agent accumulation.

3.2. Relationship between different morphological markers and phases of tumor development

We used parallels between healing wounds and cancerous tumors to establish the relationship.^{15,16} These phases were defined based on the known processes of bone remodeling markers in osteopenia and osteoporosis, as well as the development of bone metastases,^{17,18} which can be generally distinguished into three main phases:

1. Inflammation phase: The reaction of the bone microenvironment to the implantation of metastases or the therapeutic effect

2. Proliferation phase: The progression of the tumor process or focusing on the early “healing” stages, when the tissue is replaced by fibrous connective tissue
3. Recombination phase: The effect of therapy with activation of osteoblasts; in this phase, the tissue may be replaced by bone tissue, which is often unstable, or the process may return to the inflammation phase with the development of metastases.

Measurements were performed on several vertebrae, and the most typical ones were selected for illustration. [Figure 3](#) displays the time sequences of marker values in the Spine-1 observation: Arcela (A), Black Caldera (B), and Hilliness (C).

The Hilliness window initially ranged from 9 to 17 but decreased to 10 – 12. Meanwhile, Caldera generally increased and then decreased. Notably, immediately after the start of medication (palbociclib), the Arcela growth value increased from 6.7 to 11.7; this phenomenon indicates a positive response to the medication. It is also evident that each time sequence reacts not only to its key phase but also to all other phases, though less actively.

The transition to phase III (in this case, the “healing” phase) does not always occur and depends on the success of treatment. [Figure 4](#) displays the disease progression in T1 sagittal Spine-2 L2. The observation interval is close to Spine-1, making it comparable.

Instead of progressing to phase III, metastasis returned to phase I, which was confirmed in all markers. Hilliness (C) was practically unchanged (between 0.14 and 0.17), with a lower intensity compared to the intervertebral disc (129 – 130 RGB). The deviations were small, resulting in a relatively “smooth” bottom. Arcela (A) decreased from 10.9 to 6.4; that is, the complexity of the structure decreased. Meanwhile, Black Caldera (B), representing areas of dark elliptical structures, increased.

An example from the “yellow” zone and the “turbulence” zone was observed in Spine-3 (T1 sagittal Th9). [Figure 5](#) displays the changes in the markers.

We observed a slight increase of Arcela (A), but it remained within a small range of values (5.2 – 7), indicating low near-constant complexity. Caldera (B) exhibited turbulent behavior, tending to increase. Hilliness (C) did not remain constant, fluctuating between 6 and 8, but remained above the intensity of the intervertebral disc. These data suggest an intermediate change in metastases (phase II) in the spine, although a stable condition was not yet observed.

[Table 1](#) presents the currently developed criteria for defining the phases. Significant deviations from the pattern should raise suspicion of exacerbations of some kind. For contrast in phase I, a decrease >25% should be considered a positive indicator. Thus, the different phases of the

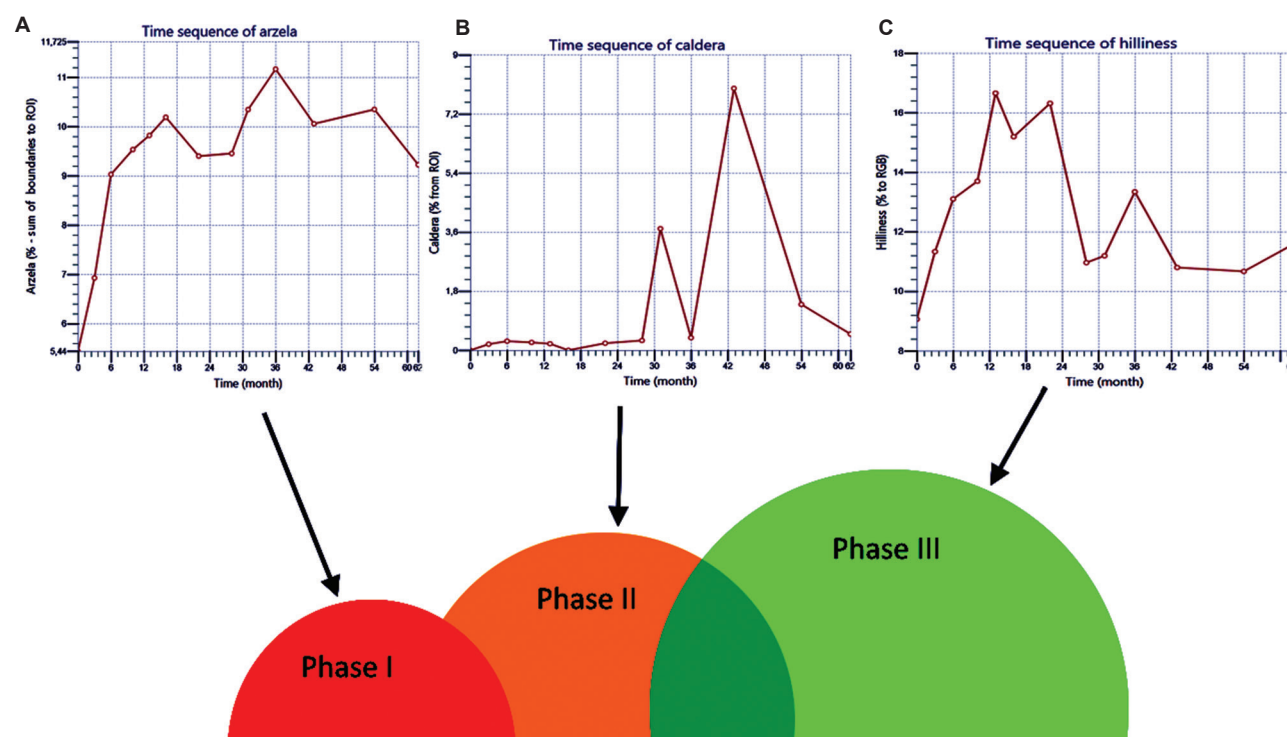


Figure 3. Metastasis regression to the “healing” phase (phase III). Arcela (A), Black Caldera (B), and Hilliness (C)

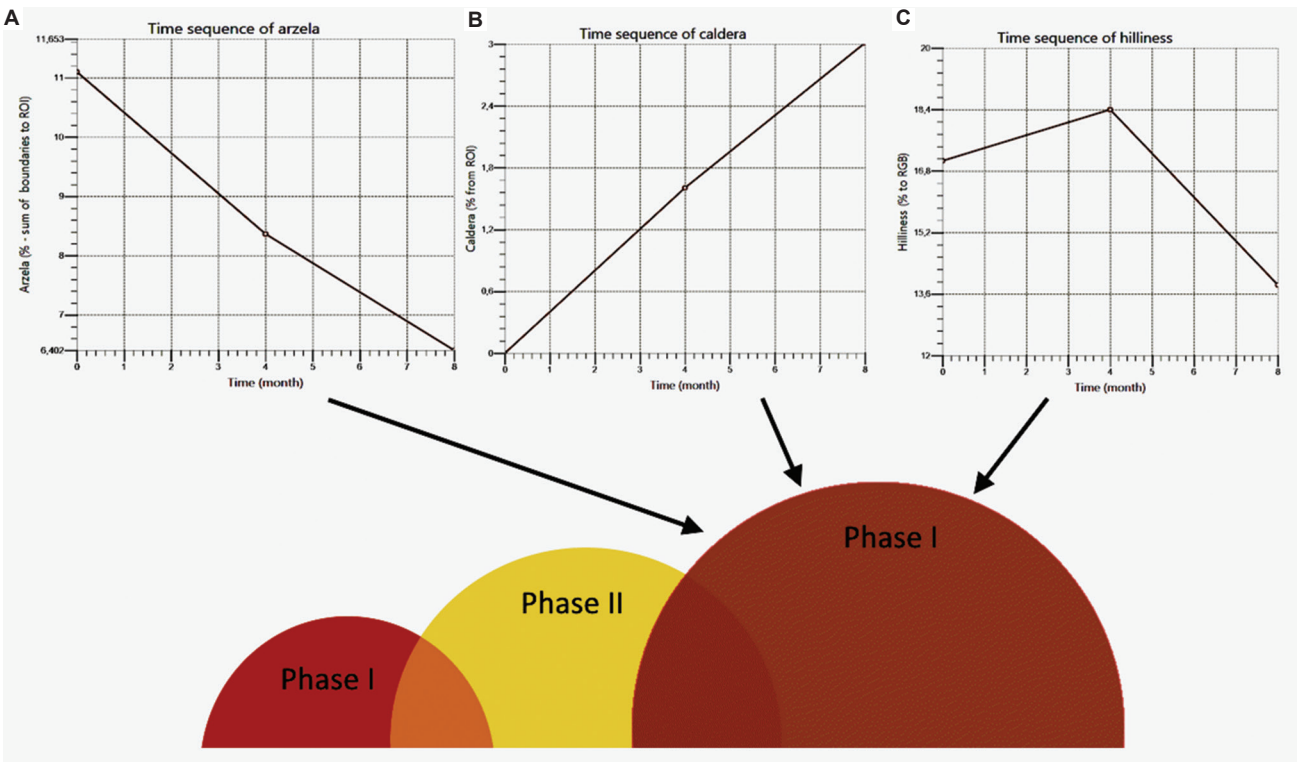


Figure 4. Metastasis has returned to phase I. Arcela (A), Black Caldera (B), and Hilliness (C)

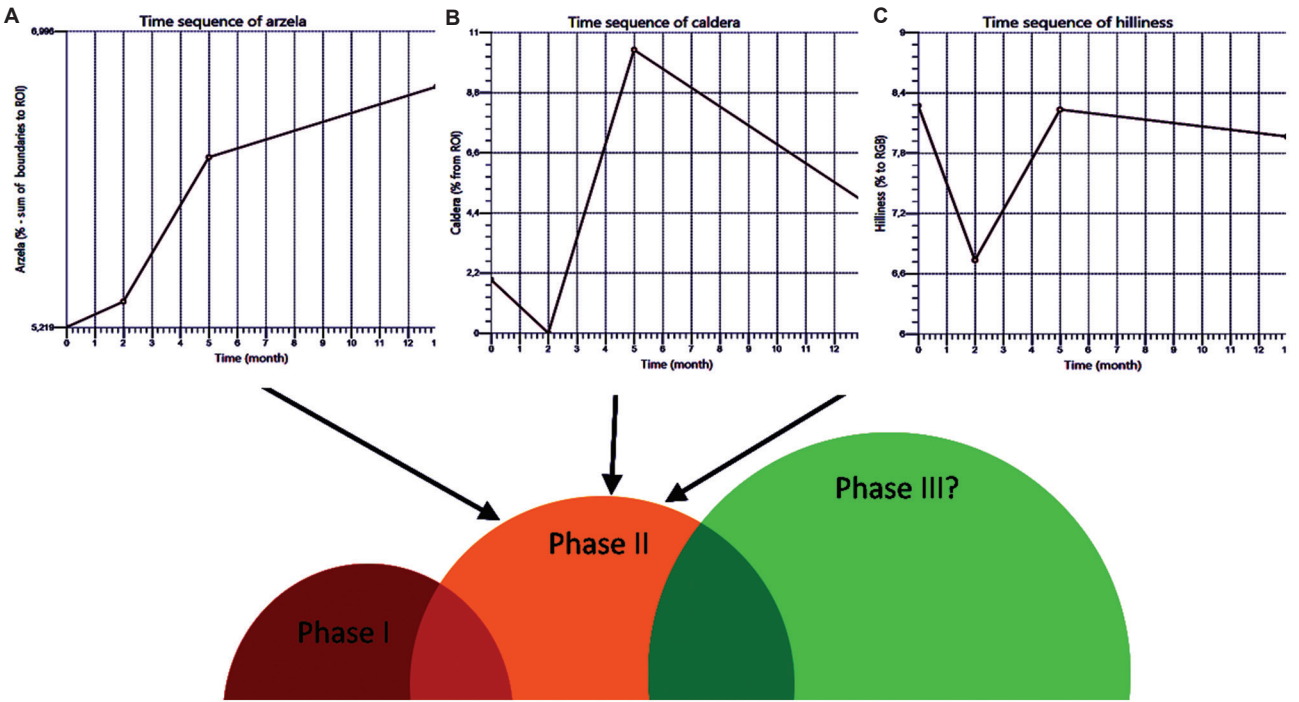


Figure 5. Metastasis in phase II. Arcela (A), Black Caldera (B), and Hilliness (C)

Table 1. Phase control in stable disease over a time interval (maximum 60 months)

Marker/ phase	Arcela (%)	Caldera (%)	Hilliness (%)	Additional information
Phase I	Growth>25	Value<5	Deviation>10	NA
Phase II	Deviation<10	Value>5	Deviation>10	NA
Phase III	Deviation<10	Value<5	Deviation<10	Intensity >~125

Note: NA: Not available.

disease are effectively monitored through the sequential application of the developed markers.

4. Discussion

The findings suggest that the selected markers, which indicate phase changes, are responsible for all the main phases of “healing,” the primary goal of this work. Such markers are especially important when the disease is asymptomatic and there are no visible signs to the radiologist. Similar coverage of the main phases of processes by markers, which physically correspond to the morphological and pathophysiological processes in vertebrae, should likely be expected in the analysis of other bones. One of the important topics for discussion is the choice of the analyzed area (ROI),¹⁹ as measurements in different planes can vary due to the internal structure of the vertebra and the asymmetric growth of tumor tissue. In this study, we focused on the sagittal section of the vertebra. For future work, we have considered the development of software for recognizing the phases of tumor process development using neural networks.²⁰ This approach is promising due to the significant non-linearity of relationships between the data and the phases, which can provide valuable insights for the doctor. Neural networks do not replace the work of the doctor but only complement it. There are also obvious difficulties in cases of sarcoidosis or deep “sclerosing.”

5. Conclusion

The recommendations for MRI T1 sagittal ROI include several positive and negative indicators. A positive indicator is a rapid rise in Arcela under the influence of the medication, as well as the presence of Black Caldera at the onset of a new medication. In addition, a long-term decrease and leveling off of Hilliness, along with the slow rise or constancy of intensity, serve as an indicator of healing.

Conversely, negative indicators include a consistently low value of mean intensity compared to the intervertebral disc, as well as low deviations from the mean intensity for ROI (Hilliness). A decrease in Arcela and a long-term increase in Black Caldera also suggest a negative response.

These recommendations provide examples of practical, numerical use of morphology based on radiologic images, which can be valuable clinically for monitoring the progression or regression of disease and treatment efficacy.

Acknowledgments

The authors would like to express their great gratitude to Prof. Dr. med. G. Hartung (MVZ, Head of oncology, Groß-Gerau, Germany) and Prof. Dr. med. S. Kümmel (Director of Breast Cancer Center, Essen, Germany) for very useful discussions on the topic.

Funding

None.

Conflict of interest

The authors declare no conflicts of interests.

Author contributions

Conceptualization: All authors

Formal analysis: All authors

Investigation: All authors

Methodology: All authors

Writing – original draft: All authors

Writing – review & editing: All authors

Ethics approval and consent to participate

Not applicable.

Consent for publication

Not applicable.

Availability of data

Data are available from the corresponding author upon reasonable request.

References

- Cardoso F, Paluch-Shimon S, Schumacher-Wulf E, *et al.* 6th and 7th International consensus guidelines for the management of advanced breast cancer (ABC guidelines 6 and 7). *Breast.* 2024;76:103756.
doi: 10.1016/j.breast.2024.103756
- Regentova OS, Solodky VA, Bozhenko VK, *et al.* Radiomic data analysis in neuro-oncology. *Bull Russ Sci Cent Roentgenol.* 2024;24:69-77.
- Jing G, Chen Y, Ma X, *et al.* Predicting mismatch-repair status in rectal cancer using multiparametric radiomics mri-based models: A preliminary study. *Biomed Res Int.* 2022;2022:6623574.
doi: 10.1155/2022/6623574

4. Hu Z, Zhuang Q, Xiao Y, *et al.* MIL normalization--prerequisites for accurate MRI radiomics analysis. *Comput Biol Med.* 2021;133:104403.
doi: 10.1016/j.compbimed.2021.104403
5. Tang WT, Su CQ, Lin J, Xia ZW, Lu SS, Hong XN. T2-FLAIR mismatch sign and machine learning-based multiparametric MRI radiomics in predicting IDH mutant 1p/19q non-co-deleted diffuse lower-grade gliomas. *Clin Radiol.* 2024;79(5):e750-e758.
doi: 10.1016/j.crad.2024.01.021
6. Sergeev NI, Kotlyarov PM, Teplyakov VV, Solodkiy VA. Peculiarities of application of diagnostic visualization methods in evaluation of treatment results of bone metastases. *Russ Electron J Radiat Diagn.* 2021;11:84-93.
doi: 10.21569/2222-7415-2021-11-4-84-93
7. Koob S, Kehrner M, Strauss A, Janzen V, Wirtz VC, Schmolders J. Knochenmetastasen-pathophysiologie, diagnostik und therapie (Teil 1) [Bone metastases-pathophysiology, diagnostic testing and therapy (part 1)]. *Z Orthop Unfall.* 2017;155(6):716-726.
doi: 10.1055/s-0043-116799
8. Ghanem N, Uhl M, Brink I, *et al.* Diagnostic value of MRI in comparison to scintigraphy, PET, MS-CT and PET/CT for the detection of metastases of bone. *Eur J Radiol.* 2005;55(1):41-55.
doi: 10.1016/j.ejrad.2005.01.016
9. Source Forge DCM4CHE. DICOM Implementation in JAVA Files. Available from: <https://sourceforge.net/projects/dcm4che/files/dcm4che3> [Last accessed on 2024 Nov 11].
10. Yue W, Hui W, Biaobiao Z, *et al.* Using radial basis function networks for function approximation and classification. *Int Sch Res Not ISRN Appl Math.* 2012;324194:34.
doi: 10.5402/2012/324194
11. Steinhauer V, Sergeev NI. Radiomics in breast cancer: In-depth machine analysis of MR images of metastatic spine lesion. *Sovrem Tehnol Med.* 2022;14(2):16-24.
doi: 10.17691/stm2022.14.2.02
12. Steinhauer V, Hartung G. Radiomics and quantitative MDA criteria in breast cancer with bone metastases by MRI: Examples of calculation algorithms and their practical use. *Sovrem Tehnol Med.* 2024;16(3):5-10.
doi: 10.17691/stm2024.16.3.01
13. Danilenko VI, Simmetriya IR. *Metodologiya I Morfogenez [Symmetry and Cancer. Methodology and Morphogenesis]*. Saarbrücken, Germany: Lap Lambert Academic Publishing; 2017. p. 85.
14. Hanahan D, Weinberg RA. Hallmarks of cancer: The next generation. *Cell.* 2011;144(5):646-674.
doi: 10.1016/j.cell.2011.02.013
15. Wietecha MS, Lauenstein D, Cangkrama M, *et al.* Phase-specific signatures of wound fibroblasts and matrix patterns define cancer-associated fibroblast subtypes. *Matrix Biol.* 2023;119:19-56.
doi: 10.1016/j.matbio.2023.03.003
16. Mccarthy-Morrogh L, Martin P. The hallmarks of cancer are also the hallmarks of wound healing. *Sci Signal.* 2020;13(648):eaay8690.
doi: org/10.1126/scisignal.aay8690
17. Koroban NV. Monitoring the effectiveness of osteoporosis therapy in HIV infection. *HIV Infect Immunosuppression.* 2017;9(2):91-94.
doi: 10.22328/2077-9828-2017-9-2-91-94
18. Karateev DE, Luchikhina EL. Current treatment for spondyloarthritis: focus on netakimab. A review. *Terapevticheskii Arkhiv (Ter. Arkh.).* 2022;18(8):8-15.
doi: 10.26442/00403660.2024.05.202794
19. Steinhauer V, Sergeev NI. Radiomics and density motphology of osteoblastic metastases of prostate cancer according to MSCCT data during therapy. *Interdiscip Sci Pract J.* 2024;18(2):62-70.
20. *Neuroph. Java Neural Network Framework. Version 2.98.* Available from: <https://neuroph.sourceforge.net> [Last accessed on 2024 Nov 11].